# Experimental Investigation of the Thermodynamics of Fe-Nb-C Austenite and Nonstoichiometric Niobium and Titanium Carbides ($T$ = 1273 to 1473 K)

K. BALASUBRAMANIAN, A. KROUPA, and J.S. KIRKALDY

The thermodynamics of Fe-Nb-C austenite and nonstoichiometric binary niobium carbide and titanium carbide in the temperature range of 1273 to 1473 K has been investigated using a dynamic gas equilibration technique. Methane-hydrogen mixtures have been used for fixing carbon potentials, and the carbon contents have been determined as dynamic weight changes *via* a sensitive Cahn microbalance. The niobium-carbon interactions, similar to the titanium-carbon interactions, are manifested as a minimum in the niobium carbide solubility in austenite, as increased amounts of dissolved carbon with niobium additions, and as the variation of solubility limit of the carbide with carbon content at high carbon levels. The results on the isoactivity measurements in the ternary Fe-Nb-C have been analyzed using the modified Wagner formalism, and the ternary interaction parameter $\varepsilon_C^{Nb}$ has been evaluated. The solubility of niobium carbide in Fe-Nb-C in austenite has been determined as the deflection in the variation of carbon content with Nb additions at constant carbon activity. The dissolution free energy of body-centered cubic (bcc) Nb in face-centered cubic (fcc) Fe has also been determined from the solubility data. Rational correlation between the dissolution free energies of transition metal solutes in fcc Fe and the group number in the Periodic Table has been shown to exist. A correlational relationship between the ternary interaction parameter and the free energy of formation of carbides has been established. These relationships are utilized in the assessment, as well as the systematization of thermodynamic data. The results on the activity-composition relationship in the binary niobium and titanium carbides have been analyzed using the sublattice-subregular model proposed by Hillert and Staffansson,[2] and the interaction parameters in the model were determined. The thermodynamic calculations based on this model and our experimental results were carried out, and very good agreement between experimental and calculated results was obtained.

## I. INTRODUCTION

IN the accompanying article,[1] the thermodynamics of Fe-Ti-C austenite and the solubility of titanium carbide in austenite in the temperature range of 1273 to 1473 K have been investigated. As a continuation, this article describes the isoactivity experiments performed to determine the thermodynamics of the Fe-Nb-C austenite phase and the nonstoichiometric niobium carbide and titanium carbide phases.

## II. EXPERIMENTAL PROCEDURE

The experimental apparatus and the dynamic equilibration technique used in this study have been described in detail in the accompanying article.[1] The starting materials for Fe-Nb alloys were high-purity iron slugs (99.995 pct) and high-purity niobium wire (99.95 pct) of about 0.25 mm in diameter. Ultrahigh-purity iron (99.999 pct) was used for making Fe-Nb alloys below 0.01 pct Nb. The compositions of alloys used in this investigation are listed in Table I. The alloys and the specimens for equilibration were made along the lines given for Fe-Ti alloys. The impurity contents in the alloys are similar in magnitude to those listed for Fe-Ti alloys in Reference 1. The carburization of pure niobium and titanium was performed using very thin foil specimens (10 to 15 $\mu$m) of these metals obtained from Alfa Products, Danvers, MA.

K. BALASUBRAMANIAN, formerly with McMaster University, is Research Scientist with the Defence Metallurgical Research Laboratories, Hyderabad 50025B, India. A. KROUPA, Research Associate, on leave from the Institute of Physical Metallurgy, Brno, Czechoslovakia, and J.S. KIRKALDY, Emeritus Professor, Department of Materials Science and Engineering and Institute for Materials Research, are with McMaster University, Hamilton, ON L8S 4L7, Canada.

Manuscript submitted April 22, 1988.

## III. EXPERIMENTAL RESULTS

### A. *Results for the Fe-Nb-C Austenite and the Austenite-Carbide Equilibrium*

The carbon contents of equilibrated Fe-Nb-C alloys at various carbon potentials are listed in Tables II through IV as well as illustrated in Figures 1 through 3. The solubility minimum in the Fe-Nb-C system occurs between 0.4 and 0.5 wt pct C in the temperature range of 1273 to 1473 K. The increase in carbon contents due to niobium additions is pronounced above 0.8 wt pct C and at higher temperatures, *i.e.*, 1373 and 1473 K. The increase in the solubility of the niobium carbide is significant at high carbon levels. The solubility limits determined by the change in slope of the carbon isoactivity lines due to niobium additions are listed in Table V in terms of the relations log [wt pct Nb] [wt pct C] and ln ($X_{Nb}X_C$). The attendant errors in the determination of the solubility of the carbide are also listed

**Table I. Composition of Fe-Nb Alloys (Wt Pct Niobium)***

| | |
|---|---|
| 1. 0.005 pct | (±0.0007) |
| 2. 0.010 pct | (±0.0005) |
| 3. 0.019 pct | (±0.0005) |
| 4. 0.037 pct | (±0.0007) |
| 5. 0.054 pct | (±0.001) |
| 6. 0.072 pct | (±0.002) |
| 7. 0.092 pct | (±0.0005) |
| 8. 0.185 pct | (±0.002) |
| 9. 0.230 pct | (±0.002) |
| 10. 0.368 pct | (±0.002) |
| 11. 0.56 pct | (±0.005) |
| 12. 0.74 pct | (±0.02) |
| 13. 0.93 pct | (±0.01) |

*The numbers in the brackets refer to the spread of compositions around the mean when measured using emission spectroscopy at four different spots on the sample.

along with other values. A more detailed description of determination of the solubility limit is offered in the accompanying article.[1]

### B. *Results for the $NbC_y$ and $TiC_y$ Phases*

The results obtained for the nonstoichiometric niobium and titanium carbide phases are given as the variation of the carbon potential (gas ratio) with the composition of the carbide (carbon/metal atom ratio) at 1273 and 1473 K in Tables VI and VII and are illustrated in Figures 4 and 5. In order to achieve very low potentials, premixed hydrogen containing 50 ppm methane mixture has been used in addition to hydrogen and hydrogen-1 pct methane mixtures. The lowest achievable compositions corresponds to $y = 0.88$ in the case of $NbC_y$ and $y = 0.86$ in the case of $TiC_y$. Very thin foils of high-purity Nb and high-purity Ti (approximately 10 $\mu$m) measuring 0.03 × 0.03 m were used for carburization. A Nb sample of these dimensions weighing nearly 90 to 100 mg picks up 12 to 15 mg of carbon at stoichiometry, while a Ti sample of similar dimensions weighs 40 to 50 mg and picks up 12 to 15 mg of carbon. A weight change of 0.02 mg which can be measured translates to 0.0016 in the atom ratio $y$, which is the accuracy of the determination of the composition of the carbide. The error in the gas ratio is about 5 pct for ratios above 1.0E-04 and 10 pct for ratios below that value.

A single specimen is sufficient to access many carbon potentials for a given temperature. Since the carbides of Nb and Ti are ceramic, the specimen tends to disintegrate after about four to five equilibration runs. New samples were introduced whenever the sample disintegrated. Compacted powder pellet specimens of approximately 1 cm in diameter and 3 mm in thickness were also tried, but the inner core of the specimen took very long times (10 to 15 days) for one equilibration run. This was due to sintering of the outer layers, which effectively sealed the pores and prevented the gas (which is

**Table II. Carbon Contents of Equilibrated Fe-Nb-C Alloys ($T$ = 1273 K)**

| Gas Ratio $\times 10^{-3}$ | $a_C$ | Wt Pct Nb | | | | | | | | | | |
|---|---|---|---|---|---|---|---|---|---|---|---|---|
| | | 0.0 | 0.005 | 0.010 | 0.019 | 0.037 | 0.054 | 0.070 | 0.092 | 0.185 | 0.368 | 0.560 |
| | | Wt Pct C | | | | | | | | | | |
| 0.7 | 0.08 | 0.176 | 0.197 | 0.196 | 0.197 | 0.199 | 0.203 | 0.203 | 0.207 | 0.220 | 0.238 | 0.265 |
| 1.05 | 0.11 | 0.292 | 0.294 | 0.294 | 0.293 | 0.304 | 0.299 | 0.297 | 0.305 | 0.315 | 0.340 | 0.362 |
| 1.55 | 0.16 | 0.416 | 0.415 | 0.419 | 0.417 | 0.421 | 0.424 | 0.424 | 0.427 | 0.440 | 0.461 | 0.482 |
| 1.75 | 0.19 | 0.445 | 0.447 | 0.447 | 0.448 | 0.452 | 0.454 | 0.455 | 0.459 | 0.470 | 0.492 | 0.514 |
| 2.00 | 0.21 | 0.517 | 0.515 | 0.514 | 0.519 | 0.522 | 0.522 | 0.524 | 0.528 | 0.539 | 0.562 | 0.581 |
| 3.35 | 0.36 | 0.803 | 0.801 | 0.802 | 0.805 | 0.809 | 0.810 | 0.814 | 0.816 | 0.825 | 0.845 | 0.877 |
| 4.95 | 0.55 | 1.094 | 1.094 | 1.097 | 1.100 | 1.101 | 1.102 | 1.107 | 1.110 | 1.118 | 0.141 | 1.163 |
| 6.10 | 0.65 | 1.286 | 1.288 | 1.290 | 1.293 | 1.296 | 1.296 | 1.300 | 1.304 | 1.312 | 1.335 | 1.357 |
| 7.70 | 0.83 | 1.522 | 1.525 | 1.523 | 1.527 | 1.534 | 1.536 | 1.539 | 1.541 | 1.551 | 1.574 | 1.589 |

**Table III. Carbon Contents of Equilibrated Fe-Nb-C Alloys ($T$ = 1373 K)**

| Gas Ratio $\times 10^{-3}$ | $a_C$ | Wt Pct Nb | | | | | | | | | | |
|---|---|---|---|---|---|---|---|---|---|---|---|---|
| | | 0.0 | 0.010 | 0.019 | 0.037 | 0.054 | 0.070 | 0.092 | 0.185 | 0.230 | 0.368 | 0.560 |
| | | Wt Pct C | | | | | | | | | | |
| 0.15 | 0.03 | 0.115 | 0.114 | 0.116 | 0.113 | 0.116 | 0.116 | 0.118 | 0.127 | 0.134 | 0.148 | 0.175 |
| 0.43 | 0.086 | 0.299 | 0.303 | 0.298 | 0.302 | 0.303 | 0.307 | 0.311 | 0.322 | 0.326 | 0.342 | 0.367 |
| 0.52 | 0.105 | 0.360 | 0.360 | 0.358 | 0.363 | 0.365 | 0.369 | 0.371 | 0.382 | 0.387 | 0.401 | 0.430 |
| 0.69 | 0.14 | 0.459 | 0.461 | 0.461 | 0.465 | 0.468 | 0.470 | 0.472 | 0.482 | 0.489 | 0.503 | 0.530 |
| 0.85 | 0.17 | 0.558 | 0.556 | 0.558 | 0.561 | 0.564 | 0.567 | 0.567 | 0.580 | 0.568 | 0.601 | 0.624 |
| 1.45 | 0.29 | 0.880 | 0.880 | 0.883 | 0.887 | 0.890 | 0.890 | 0.894 | 0.905 | 0.911 | 0.925 | 0.951 |
| 2.23 | 0.45 | 1.238 | 1.240 | 1.244 | 1.249 | 1.255 | 1.258 | 1.262 | 1.271 | 1.279 | 1.294 | 1.312 |
| 2.70 | 0.54 | 1.435 | 1.435 | 1.438 | 1.442 | 1.4547 | 1.452 | 1.456 | 1.469 | 1.475 | 1.489 | 1.511 |
| 3.7 | 0.74 | 1.794 | 1.795 | 1.799 | 1.803 | 1.809 | 1.815 | 1.822 | 1.844 | 1.850 | 1.865 | 1.884 |

**Table IV. Carbon Contents of Equilibrated Fe-Nb-C Alloys ($T$ = 1473 K)**

| Gas Ratio $\times 10^{-3}$ | $a_C$ | Wt Pct Nb | | | | | | | | | | |
|---|---|---|---|---|---|---|---|---|---|---|---|---|
| | | 0.0 | 0.037 | 0.054 | 0.070 | 0.092 | 0.185 | 0.230 | 0.368 | 0.560 | 0.740 | 0.930 |
| | | Wt Pct C | | | | | | | | | | |
| 0.14 | 0.049 | 0.226 | 0.226 | 0.228 | 0.231 | 0.235 | 0.240 | 0.245 | 0.263 | 0.284 | 0.308 | 0.332 |
| 0.22 | 0.077 | 0.345 | 0.346 | 0.348 | 0.348 | 0.352 | 0.368 | 0.369 | 0.387 | 0.411 | 0.429 | 0.455 |
| 0.28 | 0.098 | 0.429 | 0.433 | 0.431 | 0.436 | 0.440 | 0.452 | 0.457 | 0.475 | 0.500 | 0.516 | 0.540 |
| 0.35 | 0.118 | 0.509 | 0.507 | 0.513 | 0.518 | 0.521 | 0.531 | 0.537 | 0.554 | 0.578 | 0.599 | 0.619 |
| 0.41 | 0.142 | 0.605 | 0.608 | 0.608 | 0.610 | 0.616 | 0.625 | 0.633 | 0.647 | 0.672 | 0.690 | 0.715 |
| 0.61 | 0.212 | 0.849 | 0.854 | 0.854 | 0.857 | 0.866 | 0.881 | 0.885 | 0.901 | 0.926 | 0.943 | 0.965 |
| 1.05 | 0.360 | 1.304 | 1.312 | 1.310 | 1.315 | 1.322 | 1.345 | 1.352 | 1.370 | 1.389 | 1.411 | 1.425 |
| 1.34 | 0.460 | 1.574 | 1.585 | 1.590 | 1.594 | 1.601 | 1.627 | 1.637 | 1.661 | 1.677 | 1.701 | 1.719 |
| 1.46 | 0.510 | 1.688 | 1.696 | 1.700 | 1.703 | 1.711 | 1.734 | 1.748 | 1.778 | 1.795 | 1.819 | 1.835 |

very lean in methane) from reaching the inner layers. Hence, foil specimens were used, even though they lasted for only a few equilibration runs. It has been found that nearly 30 to 50 hours are required for the complete carburization (close to the graphite-carbide equilibria) of 100-mg Nb foils of 10 $\mu$m in thickness. Furthermore, large changes in chemical potential of carbon were required to give significant changes in composition. As the carbon potential in the gas decreases, the carburization time increases significantly. Therefore, specimens were initially carburized to as high a carbon content as possible, and equilibration was later achieved *via* decarburization. Long equilibration times (up to 120 hours) were allowed in the initial carburization to ensure complete equilibration, and the approach to equilibration was monitored continuously by the dynamic weight changes recorded by the electrobalance.

## IV. ANALYSIS AND DISCUSSION

The results obtained from the isoactivity experiments on the Fe-Nb-C austenite have been analyzed using the modified Wagner formalism for dilute ternary solutions. Expressions relating the ternary interaction parameter $\varepsilon_C^M$ (M = Ti, Nb) with the solubility minimum and the relative increase in carbon content at constant carbon activity due to Ti or Nb additions were derived in the accompanying article. Various approximations were given depending on the concentration of the solutes and the contributions due to the binary interaction parameters. The solubility minimum which occurs between 0.4 and 0.5 wt pct C in the temperature range of 1273 to 1473 K gives the niobium-carbon interaction parameter $\varepsilon_C^{Nb}$ as −60 to −50. A more accurate value can be obtained by considering the relation between the ternary interaction

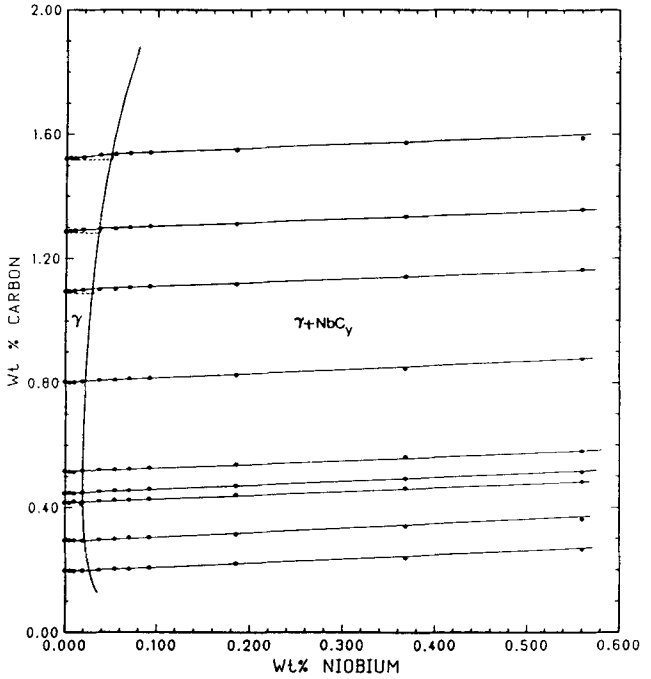


Fig. 1—The carbon contents of equilibrated Fe-Nb-C alloys ($T$ = 1273 K).

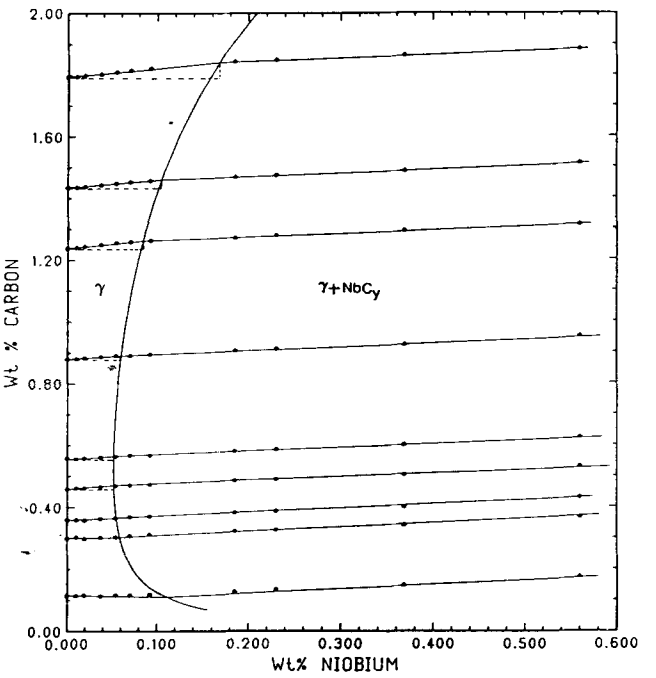


Fig. 2—The carbon contents of equilibrated Fe-Nb-C alloys ($T$ = 1373 K).

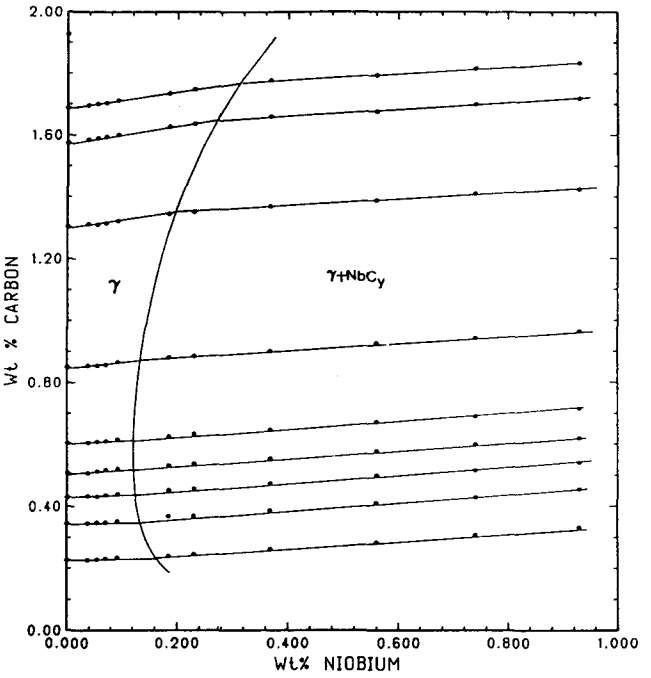


Fig. 3—The carbon contents of equilibrated Fe-Nb-C alloys ($T$ = 1473 K).

**Table VI. Variation of Composition with Carbon Potential in Niobium Carbide**

| Gas Ratio $p_{CH_4}/(p_{H_2})^2$ | C/Nb Atom Ratio $y$ | |
|---|---|---|
| 7.68E-03 | 0.986 | |
| 3.35E-03 | 0.978 | |
| 1.70E-03 | 0.970 | |
| 1.07E-03 | 0.964 | |
| 6.98E-04 | 0.958 | |
| 4.10E-04 | 0.950 | $T$ = 1273 K |
| 1.95E-04 | 0.938 | |
| 1.02E-04 | 0.927 | |
| 5.02E-05 | 0.914 | |
| 2.00E-05 | 0.896 | |
| 1.00E-05 | 0.882 | |
| 1.75E-03 | 0.983 | |
| 1.04E-03 | 0.977 | |
| 6.15E-04 | 0.970 | |
| 4.10E-04 | 0.964 | |
| 2.83E-04 | 0.958 | |
| 2.24E-04 | 0.954 | $T$ = 1473 K |
| 1.43E-04 | 0.946 | |
| 8.10E-05 | 0.935 | |
| 4.12E-05 | 0.921 | |
| 2.00E-05 | 0.905 | |
| 1.00E-05 | 0.900 | |

**Table V. Solubility of NbC in Fe-Nb-C Austenite**

| Wt Pct C | Wt Pct Nb | log [Wt Pct C · Wt Pct Nb] | Error | ln ($X_{Nb} \cdot X_C$) | |
|---|---|---|---|---|---|
| 1.53 | 0.048 | −1.13 | 0.015 | −10.79 | |
| 1.3 | 0.033 | −1.37 | 0.015 | −11.42 | |
| 1.1 | 0.029 | −1.50 | 0.015 | −11.70 | |
| 0.81 | 0.025 | −1.71 | 0.015 | −12.16 | |
| 0.52 | 0.020 | −1.99 | 0.040 | −12.80 | $T$ = 1273 K |
| 0.45 | 0.019 | −2.07 | 0.050 | −12.98 | |
| 0.42 | 0.020 | −2.08 | 0.055 | −13.00 | |
| 0.30 | 0.023 | −2.17 | 0.030 | −13.20 | |
| 0.20 | 0.027 | −2.28 | 0.025 | −13.44 | |
| 1.84 | 0.162 | −0.53 | 0.015 | − 9.52 | |
| 1.46 | 0.101 | −0.83 | 0.015 | −10.20 | |
| 1.26 | 0.081 | −0.99 | 0.020 | −10.56 | |
| 0.89 | 0.061 | −1.27 | 0.025 | −11.16 | |
| 0.56 | 0.055 | −1.51 | 0.040 | −11.69 | $T$ = 1373 K |
| 0.49 | 0.053 | −1.60 | 0.045 | −11.91 | |
| 0.37 | 0.053 | −1.71 | 0.050 | −12.14 | |
| 0.31 | 0.059 | −1.74 | 0.050 | −12.21 | |
| 0.12 | 0.110 | −1.89 | 0.030 | −12.53 | |
| 2.06 | 0.404 | −0.08 | 0.020 | − 8.50 | |
| 1.77 | 0.294 | −0.28 | 0.025 | − 8.96 | |
| 1.65 | 0.247 | −0.39 | 0.030 | − 9.20 | |
| 1.35 | 0.194 | −0.58 | 0.040 | − 9.62 | |
| 0.88 | 0.142 | −0.91 | 0.050 | −10.33 | $T$ = 1473 K |
| 0.62 | 0.123 | −1.12 | 0.055 | −10.80 | |
| 0.52 | 0.121 | −1.20 | 0.060 | −10.98 | |
| 0.45 | 0.124 | −1.26 | 0.060 | −11.11 | |
| 0.36 | 0.137 | −1.31 | 0.040 | −11.21 | |
| 0.24 | 0.170 | −1.39 | 0.030 | −11.40 | |

**Table VII. Variation of Composition with Carbon Potential in Titanium Carbide**

| Gas Ratio $p_{CH_4}/(p_{H_2})^2$ | C/Ti Atom Ratio $y$ | |
|---|---|---|
| 8.27E-03 | 0.965 | |
| 5.30E-03 | 0.960 | |
| 3.40E-03 | 0.954 | |
| 2.05E-03 | 0.949 | |
| 1.00E-03 | 0.940 | $T$ = 1273 K |
| 4.90E-04 | 0.928 | |
| 1.95E-04 | 0.913 | |
| 7.80E-05 | 0.893 | |
| 2.00E-05 | 0.871 | |
| 1.10E-05 | 0.861 | |
| 1.32E-03 | 0.956 | |
| 9.95E-04 | 0.950 | |
| 6.50E-04 | 0.942 | |
| 4.60E-04 | 0.938 | |
| 2.25E-04 | 0.930 | |
| 1.35E-04 | 0.919 | $T$ = 1473 K |
| 9.40E-05 | 0.912 | |
| 4.10E-05 | 0.889 | |
| 2.00E-05 | 0.873 | |
| 1.00E-05 | 0.864 | |

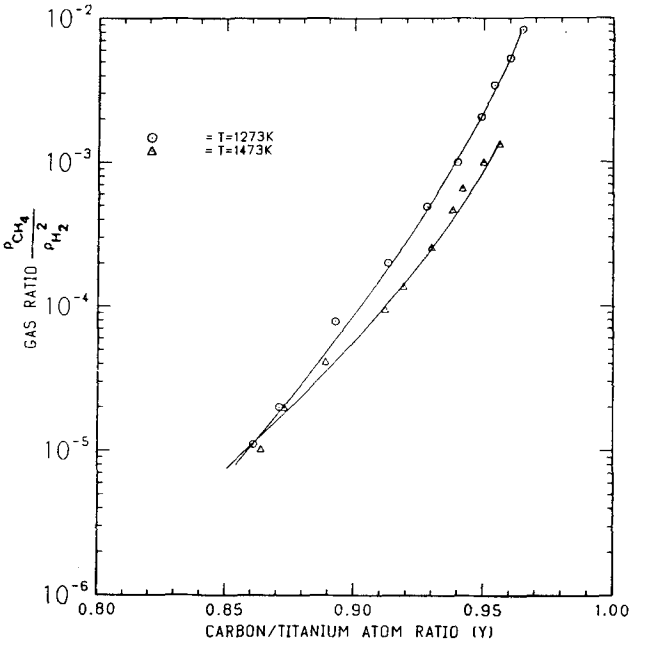


Fig. 5—Variation of composition of titanium carbide with gas ratio.

parameter and the relative increase in carbon content due to niobium additions. Rewriting Eq. [41] in Reference 1 for the Fe-Nb-C austenite, we get

$$-\varepsilon_C^{Nb} X_{Nb} = \frac{\Delta X_C}{X_C^B}[1 + X_C^B + \varepsilon_C^C X_C^B] \qquad [1]$$

where $\Delta X_C = X_C^T - X_C^B$ ($X_C^T$ is the carbon content in the ternary Fe-Nb-C system) refers to the increase in the carbon content over the binary carbon level $X_C^B$. The variation of $\Delta X_C/X_C^B[1 + X_C^B + (\varepsilon_C^C X_C^B)]$ with $X_{Nb}$ is shown in Figures 6 through 8, corresponding to 1273, 1373, and 1473 K, respectively. The slope, which is equal to $\varepsilon_C^{Nb}$, is obtained as −50 (±3), −46(±3), −43(±2), corresponding to the above three temperatures. The accuracy of the value at 1473 K is higher, as relative weight increases are higher at this temperature compared to the values obtained at the other two temperatures. The $\varepsilon_C^{Nb}$ parameter can be expressed as

$$\varepsilon_C^{Nb} = -\frac{(65{,}350 \pm 4000)}{T} + (2.5 \pm 2) \qquad [2]$$

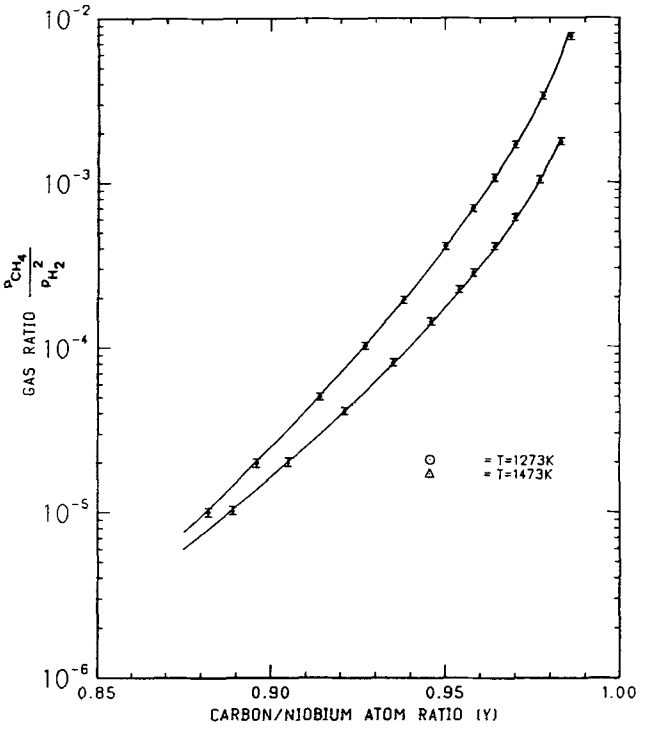


Fig. 4—Variation of composition of niobium carbide with gas ratio.

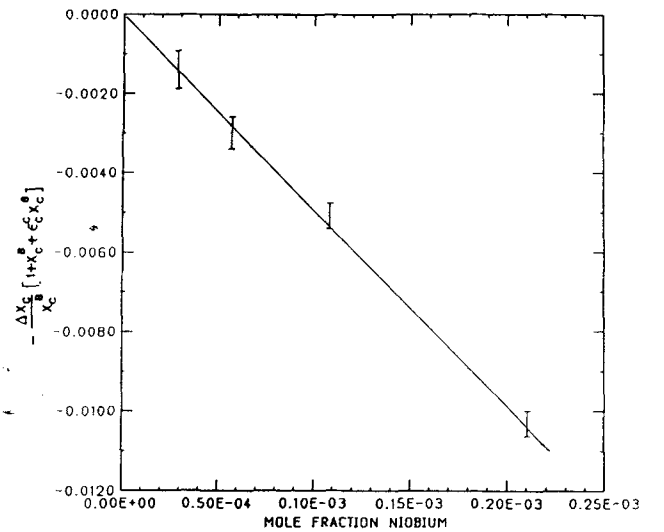


Fig. 6—Determination of niobium-carbon interaction parameter ($T$ = 1273 K).

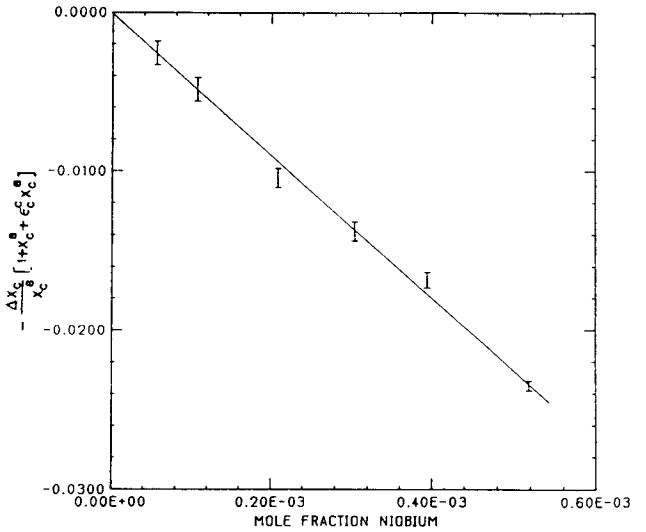


Fig. 7—Determination of niobium-carbon interaction parameter ($T$ = 1373 K).

Comparing the values for the ternary interaction parameters in the Fe-Nb-C austenites with the value $\varepsilon_C^{Ti} = -(83{,}400 \pm 4000)/T + (2.5 \pm 1.0)$ taken from the accompanying article,[1] it can be seen that $\varepsilon_C^{Ti}$ is slightly more negative than $\varepsilon_C^{Nb}$. This is in line with the free energy of formation of titanium carbide being more negative than that of niobium carbide. It can also be seen that the entropic component of both the ternary interaction parameters is small, which is in agreement with the low entropy of formation of these carbides.

The increase in the solubility of stoichiometric niobium carbide, as with the titanium case, can be described using the modified expression for the solubility of carbide in austenite as given by Eq. [46] in the previous article,[1] namely,

$$\ln [X_{Nb}X_C] = \ln K_0 - [\varepsilon_C^C + \varepsilon_{Nb}^C]X_C \qquad [3]$$

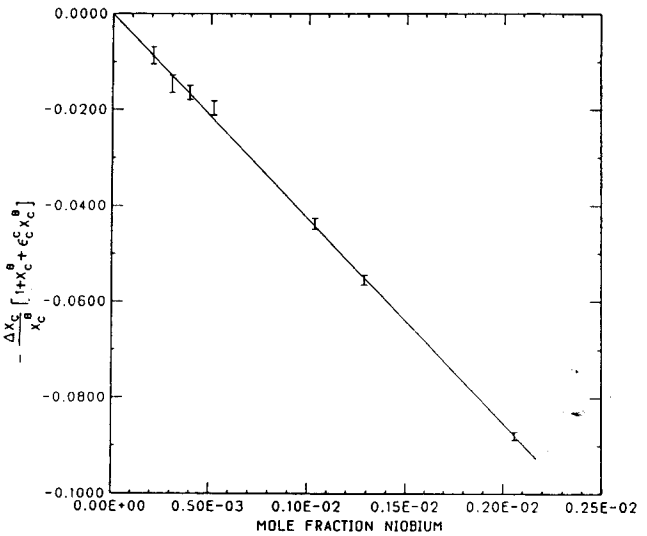


Fig. 8—Determination of niobium-carbon interaction parameter ($T$ = 1473 K).

where $K_0$ refers to the ideal solution solubility product. This can be derived *via* the free energy of formation of stoichiometric niobium carbide from pure body-centered cubic (bcc) Nb and graphite and the dissolution free energies of bcc Nb and graphite in face-centered cubic (fcc) Fe; *i.e.*,

$$RT \ln K_0 = \Delta G^\circ_{NbC} - RT \ln {}^\circ\gamma_{Nb}{}^\circ\gamma_C \qquad [4]$$

where the ${}^\circ\gamma$'s refer to the Henry's law coefficients of bcc Nb and graphite. The variations of the solubility of niobium carbide in Fe-Nb-C austenite at 1273, 1373, and 1473 K are given in Figure 9. The slopes are related to the interaction parameters given in the second term on the right-hand side of Eq. [3]. Using the following linear conversion expressions, the solubility of carbide can be expressed in terms of weight percent units as

$$X_C = \frac{\text{wt pct C}}{21.5}; \qquad X_{Nb} = \frac{\text{wt pct Nb}}{166.35} \qquad [5]$$

and

$$\log [(\text{wt pct Nb})\,(\text{wt pct C})] = \log K_0' - \left[\frac{(\varepsilon_C^C + \varepsilon_{Nb}^C)}{21.5 \times 2.303}\right] \text{wt pct C} \qquad [6]$$

$$K_0' = K_0(21.5)\,(166.35) \qquad [7]$$

where $K_0'$ stands for the ideal solution solubility product term corresponding to $K_0$ in Eq. [3]. The expression obtained in the present study is given in Table VIII.

## V. THEORETICAL RESULTS

The thermodynamic equilibria between the austenite and carbide in the Fe-Nb-C and Fe-Ti-C systems were calculated. The Hillert-Staffansson sublattice model[2] was used for the description of the phases. The experimental

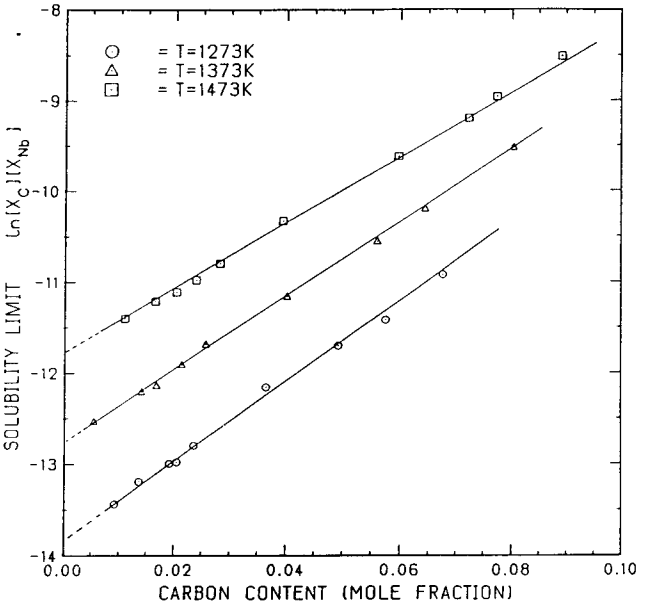


Fig. 9—Variation of solubility of NbC with carbon content.

Table VIII. Comparison of Results—Solubility Limit and Ternary Interactions in Fe-Nb-C Austenite

| | Reference |
|---|---|
| $\log$ [Wt Pct Nb] [Wt Pct C] $= -(8030/T) + 3.89 + [(1150/T) - 0.05]$Wt Pct C | this study |
| $-(4880/T) + 1.18 + [(1590/T) - 0.10]$Wt Pct C | 19, 20 |
| $-(5600/T) + 1.74 + [(1380/T) - 0.027]$Wt Pct C | 21 |
| $RT \ln {}^{\circ}\gamma_{Nb} = -27{,}950 + 13.0T$ Joules | this study |
| $-88{,}235 + 64.85T$ Joules | 19, 20 |
| $-74{,}623 + 54.20T$ Joules | 21 |
| $\varepsilon_C^{Nb} = -(65{,}350/T) + 2.5$ | this study |
| $-(87{,}620/T) + 5.0$ | 19, 20 |
| $-(77{,}220/T) + 1.3$ | 21 |

results obtained in the present study and analysis of results concerning these systems from other articles were used for reliable estimations of the thermodynamic parameters values which are necessary for the expression of the excess free energy of the above-mentioned phases.

For the calculation of the equilibria, the program TDCOMP,[3] which is based on the constrained minimization of the free-energy function of the whole system, was used. The constraints imply the mass conservation law and the conservation of the number of sites in the particular sublattices. The corresponding tielines are the results of the thermodynamic equilibria calculations for given temperatures and the composition of the whole system.

### A. *Carbide Phase $MC_y$*

The two-sublattice model in the subregular approximation was used for the description of the $MC_y$ carbide phase in the form M(C, Va), where the first sublattice is occupied by the metallic element (M = Nb or Ti) and the positions in the second interstitial sublattice are occupied by the carbon or are vacant. The positions of these vacancies are assumed to be randomly distributed in this sublattice. The assumption was made that no iron dissolves in the carbide phase. Because the dissolution of iron is actually very low, this assumption should not cause serious error in the calculated results. The molar free energy of the $MC_y$ phase existing in the NaCl structure, as given by the sublattice-subregular model, is

$$G_m = y\,{}^{\circ}G_{M:C} + (1-y)\,{}^{\circ}G_{M:Va} + RT[y \ln y + (1-y)\ln(1-y)] + y(1-y)[L_0 + L_1[y-(1-y)]] \quad [8]$$

where $y$ refers to the fraction of nonmetal atoms in the interstitial sublattice (which is the same as $y$ in the formula $MC_y$), ${}^{\circ}G_{M:C}$ is the free energy of the stoichiometric MC, and $L_0$ and $L_1$ are the interaction parameters describing the excess free energy of the system. The term ${}^{\circ}G_{M:Va}$ (Va = vacancy) refers to the free energy of the system when the interstitial lattice is completely vacant, *i.e.*, the free energy of niobium in the pure fcc state. The partial molar expressions are obtained as

$$\bar{G}_C = [{}^{\circ}G_{M:C} - {}^{\circ}G_M^{fcc}] + RT \ln\left[\frac{y}{1-y}\right] + {}^{E}\bar{G}_C \quad [9]$$

$$\bar{G}_M = {}^{\circ}G_M^{fcc} + RT \ln(1-y) + {}^{E}\bar{G}_M \quad [10]$$

where ${}^{E}\bar{G}_C$ and ${}^{E}\bar{G}_M$ refer to the partial molar excess free energies which are given below:

$${}^{E}\bar{G}_C = -L_0(2y-1) - L_1(6y^2 - 6y + 1) \quad [11]$$

$${}^{E}\bar{G}_M = y^2[(L_0 - L_1) + 2L_1(2y-1)] \quad [12]$$

It is to be noted that the functions multiplying the interaction parameters in Eq. [11] are the first- and second-order Legendre polynomials in $y$ and are orthogonal in the range zero to one. In Eq. [12], the function ${}^{E}G_M/(y^2)$ is also expressed in terms of Legendre polynomials. The constant term $(L_0 - L_1)$ becomes the coefficient of the zeroth order polynomial, $P_0 = 1$, while $2L_1$ is the coefficient of the first-order polynomial $P_1 = (2y - 1)$. Orthogonal polynomials remove the ill-conditioning associated with curve-fitting procedures and assure that the coefficients are also uncorrelated.[4] Moreover, the predominant contributions come from the leading terms, unlike the case wherein the excess free energies are expressed as an ordinary power series.

### B. *Analysis of the $NbC_y$ Phase*

The thermodynamics of cubic $NbC_y$ has not yet been adequately investigated by experiment. Most of the studies are confined to the calorimetric determination of integral properties and heat capacities of essentially stoichiometric phases. There have been only two experimental investigations pertaining to the variation of partial molar free energies, namely, the high-temperature (2300 to 2500 K) vapor pressure measurements by Storms *et al.*[5] and the electromotive force (EMF) study by Hong *et al.*[6] in the temperature range of 1100 to 1350 K. The carbon activity-composition measurements made in the present study complement the niobium activities determined in the other two studies. The results from all three data sets have been used in optimizing the parameters in the sublattice model.

The carbon activity measurements were made at 1273 and 1473 K in the present study. These measurements could not be used independently to determine the parameters, as the temperature dependence of various parameters could not be satisfactorily evaluated from this limited and relatively low temperature data. The $NbC_y$ phase is stable up to 4300 K, and hence, it is necessary to include the only available high-temperature vapor pressure data in the evaluation of the parameters. The niobium activity data from the vapor pressure measurements by Storms *et al.*[5] and Hong *et al.*[6] are listed in Table IX. The parameters in the sublattice model (Eqs. [11] and [12])

**Table IX. Niobium Activity Data from Vapor Pressure and EMF Studies**

$\log a(\text{Nb}) = A + B/T$

| Vapor Pressure Measurements (2300 to 2500 K) | | | EMF Measurements (1100 to 1350 K) | | |
|---|---|---|---|---|---|
| $y$ in NbC | $A$ | $B$ | $y$ in NbC | $A$ | $B$ |
| 0.667 | −0.6913 | 1059 | 0.720 | 1.927 | −4358 |
| 0.696 | −1.1440 | 1884 | 0.760 | 1.537 | −4246 |
| 0.700 | −1.0426 | 1554 | 0.810 | 2.441 | −5915 |
| 0.752 | −0.3915 | − 701 | 0.860 | 2.610 | −6770 |
| 0.753 | −0.3370 | − 720 | 0.910 | 1.608 | −6772 |
| 0.837 | −0.7136 | −1203 | 0.956 | 1.199 | −7494 |
| 0.842 | −0.1584 | −2547 | 0.980 | 0.674 | −7872 |
| 0.950 | −0.3119 | −4200 | — | — | — |
| 0.965 | −0.5915 | −3956 | — | — | — |
| NbC + C | −0.4298 | −8147 | — | — | — |

| | | References |
|---|---|---|
| $^{\circ}\Delta G_{\text{NbC}}$ | $-146{,}650 - 1.76T$ J/mol Nb | 8, 7 |
| $RT \ln [a(\text{Nb})]$ at NbC + C | $-155{,}985 - 8.23T$ Joules | vapor pressure, 5 |
| $RT \ln [a(\text{Nb})]$ at $y = 0.98$ | $-150{,}720 + 12.9T$ Joules | EMF, 6 |

were evaluated at three temperatures, 1273, 1600, and 2400 K, using selected data from all of the investigations. A linear temperature dependence of these parameters was then obtained from the evaluations at these three temperatures. For 1273 K data was used from all of the investigations except those corresponding to $y = 0.72$, 0.76 from the EMF study, the reason for the deletions being the uncertainty over the partial molar entropies.[6] At 1600 K, there is good agreement between the two niobium data sets, and hence, all of the data points were used. At 2400 K, only the vapor pressure data were used, as most of the EMF measurements could not be satisfactorily extrapolated from 1200 to 2400 K. Figures 10 and 11 show the variation of partial molar free energy of niobium as a function of composition at 1273 and 2400 K. The evaluated parameters are given in Table XIV, along with the free energy of formation of stoichiometric NbC taken from Hultgren *et al.*[7] and the lattice stability ($^{\circ}G^{\text{fcc}} - {}^{\circ}G^{\text{bcc}}$) values given by Kaufman and Nesor.[8]

The NbC phase is in equilibrium with pure graphite at the carbon-rich boundary. The carbon-rich phase boundary is determined as $y = 0.99 \pm 0.005$ at 1273 K in the present study using the hydrogen-methane gas mixture. The partial molar free energy of niobium at that boundary should be very close to the free energy of formation of the stoichiometric compound, which is known

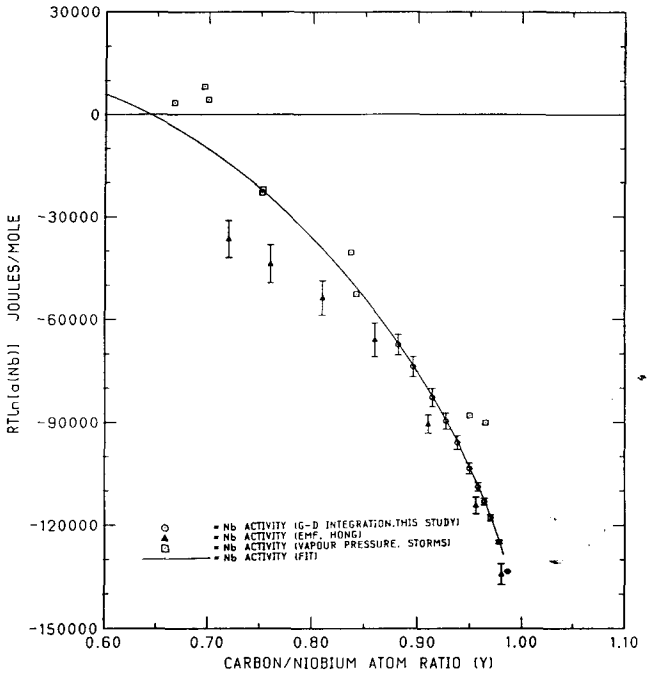


Fig. 10—Variation of partial molar free energy of niobium in niobium carbide ($T$ = 1273 K).

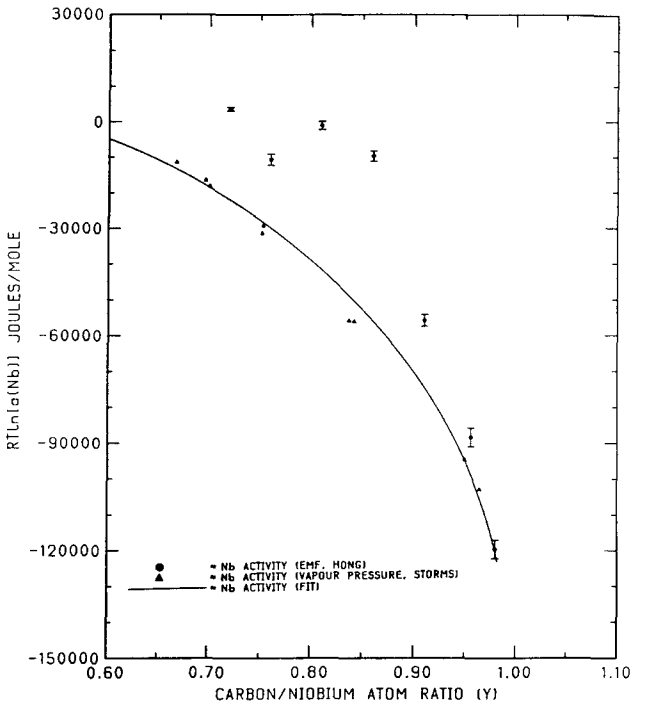


Fig. 11—Variation of partial molar free energy of niobium in niobium carbide ($T$ = 2400 K).

from independent calorimetric studies and lattice stability values to be $-146{,}650 - 1.76T$ Joules/mol Nb. The EMF study gives good agreement with the calorimetric value for the composition $y = 0.98$, while the vapor pressure measurement over NbC + C by Storms *et al.*[5] gives a slightly more negative value, as shown in Table IX.

### C. *Analysis of the $TiC_y$ Phase*

There have been a few low-temperature (1050 to 1473 K) studies[9–12] and one high-temperature (1900 K) vapor pressure measurement by Storms[13] on the partial molar free energies of titanium and carbon in the $TiC_y$. Table X outlines the summary of these experimental investigations on the partial molar free energies of binary titanium carbide phase. Even though data on both the titanium and carbon activity are available from these five investigations, there is considerable discrepancy between the activity-composition relationships obtained from all of these investigations. Hence, critical assessment of data using thermodynamic models is necessary. The thermodynamics of this phase has been analyzed by Teyssandier *et al.*,[14] Kaufman and Agren,[15] and Uhrenius.[16] Teyssandier *et al.* used the substitutional regular solution model with a Redlich-Kister expansion for the excess free energy, while Uhrenius and Agren used the sublattice subregular model suggested by Hillert and Staffansson[2] for analyzing the $TiC_y$ phase. Of all the available experimental results, only the vapor pressure measurements by Storms[13] and the low-temperature EMF measurements by Koyama and Hasimoto[12] have been found to be consistent with the phase diagram in the assessments by the above-mentioned authors. As there were insufficient data at high temperatures, Kaufman and Agren used the high- and low-carbon phase boundaries of the $TiC_y$ phase together with Storms' data at 1900 K to evaluate the parameters.

The carbon activity as a function of temperature and composition has been measured using the gas equilibration technique by Alekseev *et al.*[9] and Grieveson.[10] Figure 12 shows the variation of the partial molar free energy of carbon in $TiC_y$ at 1273 K along with predictions by Teyssandier *et al.*[14] and Kaufman and Agren.[15] The activity values of Grieveson are very high compared to those of Alekseev, and both these data sets give higher values compared to the results in the present study. One of the reasons for this discrepancy could be insufficient time for equilibration and possible sintering of the powder compacts used as samples in the earlier studies which reduce the permeability of the gas mixture. As mentioned in the earlier section, nearly 30 to 50 hours are

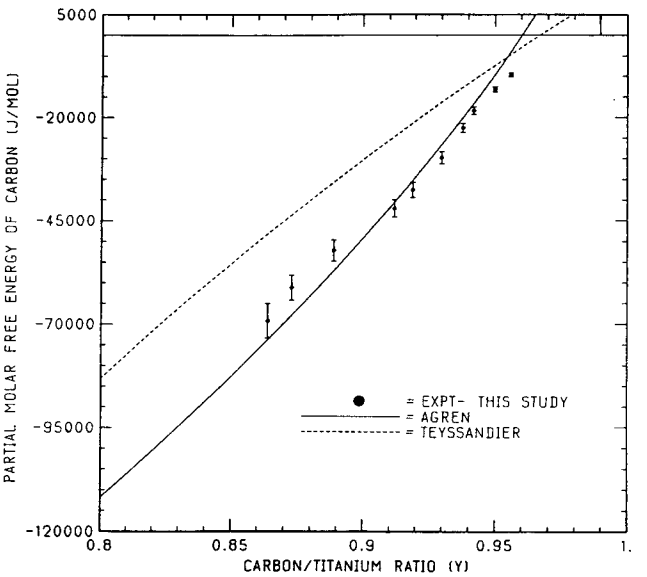


Fig. 12—Variation of partial molar free energy of titanium in titanium carbide ($T$ = 1273 K).

required for the carburization of a 50-mg foil of about 10 $\mu$m in thickness. Moreover, very low carbon potentials (Figures 4 and 5) are required to attain compositions below $y = 0.85$, and gas equilibration techniques are not well suited for such low potentials. The data obtained in the present study is in fair agreement with the predictions of Kaufman and Agren at compositions of above $y = 0.9$, but the difference increases as carbon content is decreased. Teyssandier *et al.* used the titanium activity data given by Storms at 1900 K and Koyama at 853 K to obtain the parameters in their substitutional regular solution model. Their predictions are higher than those given by Kaufman and Agren, and the discrepancy is larger at lower carbon contents. As Kaufman and Agren used the low-carbon phase boundary in addition to Storms titanium activity data and the high-carbon phase boundary for evaluating the parameters, their predictions should be more reliable at low carbon levels. As the accuracy of the data obtained at carbon levels below $y = 0.9$ is limited and as the data at higher carbon levels are reasonably close to the predictions of the latter authors, their parameters in the sublattice model prove sufficient for the description of the data obtained in the present study. The parameters given by Kaufman and Agren are given in Table XIV along with the evaluated parameters for the $NbC_y$ phase.

**Table X. Summary of Experimental Investigations on the Partial Molar Free Energies in Binary Titanium Carbide**

| Property Measured | Composition Range | Temperature Range | Experimental Technique | Reference |
|---|---|---|---|---|
| $a_C$ | $0.70 \le y \le 0.89$ | 1173 to 1373 K | gas equation | 9 |
| $a_C$ | $0.67 \le y \le 1.0$ | 1273 to 1473 K | gas equation | 10 |
| $a_{Ti}$ | $0.69 \le y \le 1.0$ | 1045 to 1135 K | EMF | 11 |
| $a_{Ti}$ | $0.71 \le y \le 1.0$ | 853 K | EMF | 12 |
| $a_{Ti}$ | $0.54 \le y \le 0.89$ | 1900 K | vapor pressure | 13 |

D. *Analysis of the Austenite Phase*

The two-sublattice model in the subregular approximation was also used for description of austenite in the form (Fe, M) (C, Va)$_a$, where $a = 1$ for the fcc structure and M can be Nb or Ti. The molar free energy of austenite is then given by

$$\begin{aligned} G_m = {} & Y_{Fe}(1 - Y_C)^\circ G_{Fe:Va} + Y_M(1 - Y_C)^\circ G_{M:Va} \\ & + Y_{Fe}Y_C{}^\circ G_{Fe:C} + Y_M Y_C{}^\circ G_{M:C} \\ & + RT(Y_{Fe} \ln Y_{Fe} + Y_M \ln Y_M + Y_C \ln Y_C \\ & + (1 - Y_C) \ln (1 - Y_C)) \\ & + Y_{Fe}Y_M(Y_C L_{FeM:C} + (1 - Y_C)L_{FeM:Va} \\ & + Y_C \cdot (1 - Y_C) \cdot (Y_{Fe}L_{CVa:Fe} + Y_M L_{CVa:M}) \end{aligned} \quad [13]$$

where

$$L_{FeM:k} = {}^\circ L_{FeM:k} + {}^1L_{FeM:k}(Y_M - Y_{Fe}) \quad [14]$$

$$L_{CVa:i} = {}^\circ L_{CVa:i} + {}^1L_{CVa:i}(Y_C - (1 - Y_C)) \quad [15]$$

$$Y_i = \frac{X_i}{1 - X_c} \quad [16]$$

where $Y_i$ refers to the site fraction of elements in the first (Fe or Nb) and the second (C, Va) sublattice, $X_i$ are the molar fractions of the elements in the austenite, ${}^\circ G_{iVa}$ is the free energy of pure metal with an fcc structure, and ${}^\circ G_{iC}$ is the free energy of hypothetical solution when all interstitial holes are occupied by carbon. It is, of course, equal to the free energy of stoichiometric MC carbide. The values of these parameters were taken from References 7, 8, 17, and 18. Parameters $L$ describe the excess free energy and were partially estimated in the present study on the basis of experimental results similar to those in the case of carbide phase.

The experimental results in our study, together with the analysis of results obtained in other studies of these systems, were used for the estimation of the thermodynamic parameters. The value of parameter $L_{FeM:C}$ was estimated with the help of the relationship between the ternary interaction parameter $\varepsilon_C^M$ and this thermodynamic parameter. The value of the ternary interaction parameter was obtained from the articles of Ohtani.[19,20,21] The values are listed in Table VIII, together with the value obtained in the present study. There is good agreement between these values. For the estimation of the thermodynamic parameter $L_{FeM:C}$, the value of $\varepsilon_C^M$ from the present study was used. The best agreement between the calculated and experimental results was achieved for the value of the ternary interaction parameter at the lower error bound (Eq. [2]) as is given in the previous part of this study.[1] The value of the $L$ parameter corresponds to this value of $\varepsilon_C^M$ This evaluation was carried out both for the Fe-Nb-C and Fe-Ti-C systems, and the values of this parameter for the above-mentioned systems are given in Table XIV.

The parameter $L_{FeM:Va}$ was calculated on the basis of the free energy of dissolution of the metal solute M in fcc iron. The formula, relating the parameters in the expression of partial molar excess free energy in the subregular approximation and the activity coefficient in the Wagner formalism, is developed in Reference 22 for the binary Fe-M system in the form

$$RT \ln {}^\circ\gamma_M = {}^\circ L_{FeM:Va} - {}^1L_{FeM:Va} \quad [17a]$$

$$RT\varepsilon_M^M = 6 \cdot {}^1L_{FeM:Va} - 2 \cdot {}^\circ L_{FeM:Va} \quad [17b]$$

where ${}^\circ L$ and ${}^1L$ are defined by Eq. [14].

The detailed analysis of the values of free energy of dissolution obtained and the recommended value which was used for estimation of the above-mentioned parameter $L$ is given in Reference 1 for the Fe-Ti-C system and in Section E of the present article for the Fe-Nb-C system. The values of parameter $L$ for both systems are given again in Table XIV. For the Fe-Nb-C system, there are no reliable values of the ternary interaction parameter $\varepsilon_{Nb}^{Nb}$ and the coefficients ${}^\circ L$ and ${}^1L$ from previous articles, and therefore, no concentration dependence of this parameter was taken into account.

The results of the calculations are shown in Figures 13 through 15 for the Fe-Nb-C system. It is seen that the agreement between the calculated and experimental results obtained in the present study is very good, especially for the ternary parameter values taken from the lower error bound, as are given in Eq. [2]. This result crosschecks the experimentally evaluated parameters of the modified Wagner formalism $\varepsilon_C^M$ and $RT \ln {}^\circ\gamma_M$ with the help of an estimation of the thermodynamic parameters $L$ for the Hillert-Staffansson sublattice model. The results suggest good reliability of the Wagner parameter values calculated from the experimental results.

E. *Free Energy of Dissolution of Bcc Nb in Fcc Iron*

The dissolution free energy of niobium in fcc iron is, in principle, determinable from the thermodynamics of the fcc phase in the binary Fe-Nb system. However, the experimental information on this phase is lacking. The available information in the literature[8,23] is limited to the values determined *via* computer calculations using

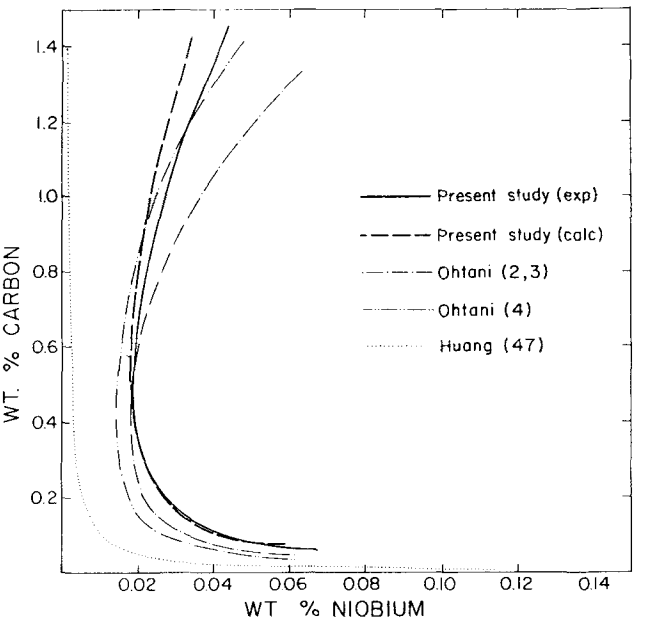


Fig. 13—Comparison of solubility limits of NbC ($T$ = 1273 K).

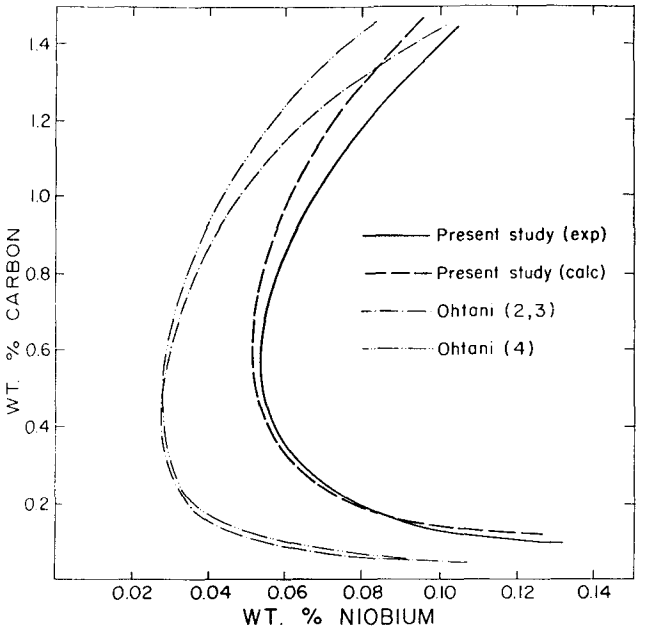


Fig. 14—Comparison of solubility limits of NbC ($T$ = 1373 K).

the experimental phase diagram and thermodynamic data on liquid and bcc phases. One such effort by Kaufman and Nesor[8] predicts an ideal solution behavior for Nb (reference state fcc Nb) in fcc Fe, while the calculations of Paul and Swartzendruber[23] show positive deviations from ideality. A limited experimental investigation by Hawkins[24] shows small negative deviations from ideality.

There have been many investigations[25–31] on the solubility of NbC in Fe-Nb-C austenite at carbon levels below 0.2 wt pct C. As the effect of solute interactions are negligible at these carbon levels, results from these investigations have been expressed in the form of the ideal solution solubility product relationship. The solubility of NbN has also been investigated[32–35] by many authors.

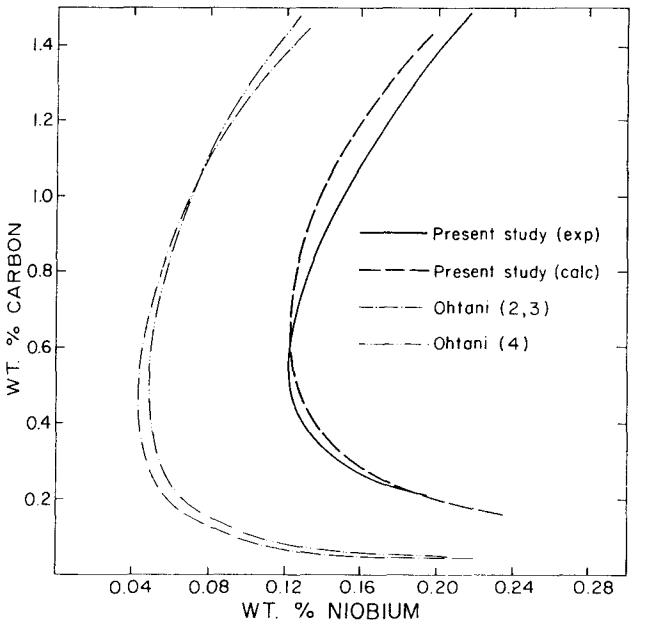


Fig. 15—Comparison of solubility limits of NbC ($T$ = 1473 K).

The free energy of dissolution of bcc Nb in fcc iron could be obtained from these solubility measurements involving NbC and NbN in austenite. The results obtained from such an exercise, together with the values obtained by Ohtani *et al.*[19,20,21] and those obtained in the present study, are given in Table XI.

It can be seen from Table XI that values ranging from −12 to +18 KJ/mole are obtained. Ohtani *et al.*'s[19,20,21] results range from −5 to +8 KJ/mole, while the present study gives −10 (+1.5) KJ/mole in the temperature range of 1273 to 1473 K. A few other features can be inferred from the results illustrated in Table XI. First, both the enthalpic and entropic components exhibit a wide range of values, and second, the values determined from the NbN solubility are more consistent than those determined from the NbC solubility. In fact, the Fe-Nb-N system[35] satisfies all of the assumptions made in the derivation of the solubility relationship for ideal solution. Most of the studies were carried out close to and at 1 atm N, and hence, the precipitate is close to stoichiometry, while only studies done at very high carbon levels, like the present one, satisfy this requirement in the Fe-Nb-C system. The contributions arising from solute interactions are minimal due to very low concentrations of N in austenite, and hence, the solubility limits in Fe-Nb-N austenite reflect the dissolution characteristics of N and Nb to a greater degree than the corresponding carbon austenite. Therefore, the values obtained from NbN studies should be more reliable. Thus, the dissolution free energy of niobium in iron should be around −10 to −15 KJ/mole in the temperature range of 1273 to 1473 K. An average of the values obtained from the consistent NbN solubility results[33,34,35] is recommended as the free energy of dissolution of bcc niobium in fcc iron, namely,

$$RT \ln {}^{\circ}\gamma_{Nb}^{bcc} = -25{,}500 + 10.9T \quad \text{Joules/mol Nb} \qquad [18]$$

### F. *Correlational Relationships and the Dissolution Free Energy of Solutes*

In Section E, we determined the dissolution free energy of bcc Nb in fcc iron from the solubility studies. The negative deviations from ideality that are predicted by such evaluations can be rationalized by considering the solution behavior of other transition metals in fcc iron. A reasonable value for the Henry's law coefficient, or a parameter describing the excess free energy of mixing of fcc Fe-Nb phase, can be obtained *via* suitable Periodic Table correlations. Hume-Rothery[36] found correlations between the size, the electronegativity difference, and the position of the solute in the Periodic Table on the one hand with the constitution of Fe-M systems on the other. The extent of the fcc phase, the tendency to form intermetallic phases, and the relative effects of solute in stabilizing the fcc or bcc phase correlated well with the size factor and the position of the solute relative to iron in the Periodic Table. A similar correlation can be shown to exist between the free energy of dissolution (Henry's law coefficient) and the aforementioned factors. The thermodynamics of the fcc phase in many binary Fe-M systems have been analyzed using

**Table XI. Dissolution Free Energy of Bcc Niobium from Solubility Studies**

$^{\circ}G_{NbC} - {}^{\circ}G_{Nb}^{bcc} - {}^{\circ}G_{gr} = -137{,}650 + 1.78T$ J/Mole of Nb[7]
$RT \ln {}^{\circ}\gamma_C = 44{,}180 - 17.7T$ J/Mole of C[46]

| Solubility Limit log [Nb] [X] = A + B/T | | $RT \ln {}^{\circ}\gamma_{Nb}$ (Joules) | | | |
|---|---|---|---|---|---|
| A | B | 1273 K | 1373 K | 1473 K | Reference |
| | | Fe-Nb-C | | | |
| 2.90 | − 7500 | 2557 | 5749 | 8940 | 25 |
| 3.18 | − 7700 | − 438 | 2218 | 4873 | 26 |
| 3.42 | − 7900 | − 2458 | − 262 | 1933 | 27 |
| 3.04 | − 7290 | − 4875 | − 1952 | 971 | 28 |
| 3.70 | − 9100 | 13,693 | 15,352 | 17,013 | 29 |
| 4.37 | − 9290 | 1000 | 1337 | 1754 | 30 |
| 3.31 | − 7970 | 1563 | 3970 | 6376 | 31 |
| 1.18 | − 4880 | − 5684 | 800 | 7285 | 19, 20 |
| 1.74 | − 5600 | − 5633 | − 214 | 5206 | 21 |
| 3.89 | − 8030 | −11,425 | −10,130 | − 8832 | this study |
| | | Fe-Nb-N | | | |
| 3.79 | −10,150 | − 7604 | − 6766 | − 5707 | 32 |
| 4.04 | −10,230 | −12,166 | −11,807 | −11,226 | 33 |
| 2.80 | − 8500 | −15,067 | −12,333 | − 9378 | 34 |
| 4.2 | −10,000 | −11,840 | −10,960 | −10,070 | 35 |

techniques such as computer coupling of thermochemistry and phase diagrams in recent years. The results obtained by such techniques[37–45] are given in the form of regular solution parameters, and the dissolution free energy of the various solutes can be extracted from these parameters[35] (Table XII). The size factor is defined as the difference in the atomic diameters of iron and the solute atom in 12-fold coordination. The calculated diameters and the size factors for various solutes are given in Table XIII. The correlation of the dissolution free energy of fcc Nb in fcc iron with the size factor and the position of the solute in the periodic table is shown in Figures 16 and 17. The correlation with the latter is striking, and hence, as a first approximation, the valence effects of solutes can be considered to be the predominant factors controlling the thermodynamics of dissolution. However, the limited correlation with the size factor is also significant, and the size effects become equally important for solutes farther away from iron in the Periodic Table. Niobium belongs to the same group as vanadium (Group VA) and its size factor is closer to that of titanium (Table XIII). Hence, an average of the values for titanium and vanadium should be a reasonable estimate for the dissolution free energy of niobium. The value

**Table XII. Excess Free Energies of Fcc Phases in Fe-M Systems**

Excess Free Energy $= X_M(1 - X_M)\,[{}^{\circ}L + {}^{1}L(X_M - X_{Fe})]$ Joules/Mole
$RT \ln {}^{\circ}\gamma_M = {}^{\circ}L + {}^{1}L$ Joules/Mole

| System | $^{\circ}L$ | $^{1}L$ | $RT \ln {}^{\circ}\gamma_M$ | $({}^{\circ}G_M^{fcc} - {}^{\circ}G_M^{bcc})$ | Reference |
|---|---|---|---|---|---|
| Fe-Zn | 6940 + 5.16T | 0 | 6940 + 5.16T | − 1045 + 0.84T | 37 |
| Fe-Cu | 48,206 − 8.45T | − 5920 + 5.02T | 54,125 − 13.46T | − 6275 + 3.35T | 38 |
| | 53,360 − 12.63T | 11,512 − 7.10T | 41,850 − 5.53T | | 39 |
| Fe-Ni | 18,300 − 5.15T | −14,310 − 5.15T | 32,610 − 12.81T | − 5650 − 3.35T | 38 |
| | 14,240 − 2.82T | 11,512 − 7.10T | 41,850 − 5.53T | | 40 |
| Fe-Cr | 10,830 − 7.45T | 1410 | 9420 − 7.45T | 10,460 + 0.63T | 41 |
| Fe-Mn | − 5980 + 2.84T | 0 | − 5980 + 2.84T | − 1800 + 1.28T | 43 |
| Fe-V | −18,180 + 1.16T | 0 | −18,180 + 1.16T | 9000 + 3.56T | 44 |
| Fe-Ti | −31,000 | 11,506 | −42,506 | − 1005 + 3.76T | 45 |
| | −21,966 | 11,506 | −33,372 | | 46 |
| Fe-Mo | 28,347 − 17.7T | 0 | 28,347 − 17.7T | 10,460 + 0.63T | 42 |
| Fe-Nb | 0 | 0 | 0 | 9000 + 3.56 | 46 |

Note: The values of $RT \ln {}^{\circ}\gamma_M$ given in this table are with respect to the fcc state of the solutes. To obtain similar values with respect to the bcc state, lattice stability values $({}^{\circ}G_M^{fcc} - {}^{\circ}G_M^{bcc})$ must be added to the above $RT \ln {}^{\circ}\gamma_M$ values.

**Table XIII. Calculated Atomic Diameters (Coordination Number = 12)**

| Metal | Crystal Structure | Lattice* Parameter (KX Units) | Atomic Diameter (KX Units) | $d - d$ Fe-M (KX Units) |
|---|---|---|---|---|
| Cu | fcc | 3.6074 | 2.5508 | +0.0226 |
| Ni | fcc | 6.5166 | 2.4866 | +0.0868 |
| Co | fcc | 3.5370 | 2.5010 | +0.0724 |
| | | 3.5540 | 2.5130 | +0.0604 |
| Fe | fcc | 3.6394 | 2.5734 | 0.0 |
| | bcc | 2.8606 | 2.4473 | |
| | bcc (1667 K) | 2.9263 | 2.5342 | |
| Mn | fcc (1368 K) | 3.8546 | 2.7256 | −0.1522 |
| | bcc (1407 K) | 3.0744 | 2.7424 | |
| Cr | bcc | 2.8788 | 2.5679 | −0.0055 |
| V | bcc | 3.0286 | 2.6956 | −0.1222 |
| Ti | bcc (1173 K) | 3.3065 | 2.9435 | −0.3701 |
| | hcp | 2.9504(a) | 3.0054 | −0.4320 |
| | | 4.6833(c) | 3.0623 | −0.4889 |
| Mo | bcc | 3.1405 | 2.8013 | −0.2279 |
| Nb | bcc | 3.2940 | 2.9382 | −0.3648 |
| W | bcc | 3.1586 | 2.8174 | −0.2440 |

*Taken from Ref. 51.

obtained in such a manner is around −15 KJ/mol (for bcc Nb in fcc Fe), which is close to the value recommended above in Eq. [18].

## VI. COMPARISON OF RESULTS

Ohtani *et al.*[19,20,21] reported increased solubility of niobium carbide at carbon levels above 0.5 wt pct C and reported the solubility results in the form of Eq. [6]. They obtained these results both from the experimental and theoretical approach. The Henry's law coefficient for bcc Nb in fcc Fe and the niobium-carbon ternary interaction parameter can be extracted from the first and second terms in Eq. [6] to facilitate comparison of the results from these studies. The comparison is given in Table VIII.

It can be seen from Table VIII that the ternary interaction parameter for niobium-carbon interaction obtained from the results of Ohtani *et al.* is slightly more negative compared to the value obtained in this study, but the values are well within 10 pct of each other. It is worth noting that the entropy terras of the interaction parameters are very small in both investigations. The solubility limits from the two studies, which are compared in Figures 13 through 15, show fair agreement at lower temperature, but the difference between the four data sets (our experimental and calculated and Ohtani *et al.*'s experimental and calculated from References 19 through 21) widen with increasing temperature. The solubility given by Ohtani *et al.* is smaller than obtained in the present study. The reason for this discrepancy is to be found in the leading term of Eq. [6], which defines the solubility product for an ideal solution that neglects the solute interaction. On comparing the value for this term from the three studies (Table VIII), it can be seen that Ohtani *et al.*'s results [$(-4880/T) + 1.18$ and $(-5600/T) + 1.74$, respectively)] are marked by smaller (absolute value) enthalpic and entropic contributions compared to those obtained in the present study, namely,

**Table XIV. Thermodynamic Interaction Parameters and Free-Energy Values for Fe-Nb-C and Fe-Ti-C Systems (All Values in Joules/Mole of Metal)**

| Parameter | $NbC_y$ Phase | Reference | $TiC_y$ Phase | Reference |
|---|---|---|---|---|
| ${}^{\circ}G_{MC} - {}^{\circ}G_M^{fcc} - {}^{\circ}G_{gr}$ | −146,650.0 − 1.76$T$ | 7 | −187,295.0 + 10.58$T$ | 7 |
| ${}^{\circ}G_M^{fcc} - {}^{\circ}G_M^{bcc}$ | 8995.0 + 3.56$T$ | 8 | − 1004.0 + 3.77$T$ | 8 |
| $L_0$ | − 42,625.0 + 4.42$T$ | this study | − 67,365.0 + 1.50$T$ | 15 |
| $L_1$ | −114,525.0 + 33.58$T$ | this study | −162,340.0 + 46.15$T$ | 15 |
| | Austenite phase | | | |
| | Nb | | Ti | |
| ${}^{\circ}L_{FeM:C}$ | −421,302.3 + 54.106$T$ | this study | −579,859.0 + 53.772$T$ | this study |
| ${}^{\circ}L_{FeM:Va}$ | − 34,495.0 + 7.25$T$ | this study | − 62,637.0 + 18.11$T$ | this study |
| ${}^{1}L_{FeM:Va}$ | 0.0 | | − 2051.0 + 6.04$T$ | this study |
| ${}^{\circ}L_{CVa:M}$ | − 42,625.0 + 4.42 | this study | − 67,365.0 + 1.50$T$ | 15 |
| ${}^{1}L_{CVa:M}$ | −114,525.0 + 33.58$T$ | this study | −162,340.0 + 46.15$T$ | 15 |
| ${}^{\circ}L_{CVa:Fe}$ | − 28,700.0 − 5.6$T$ | 21 | | |

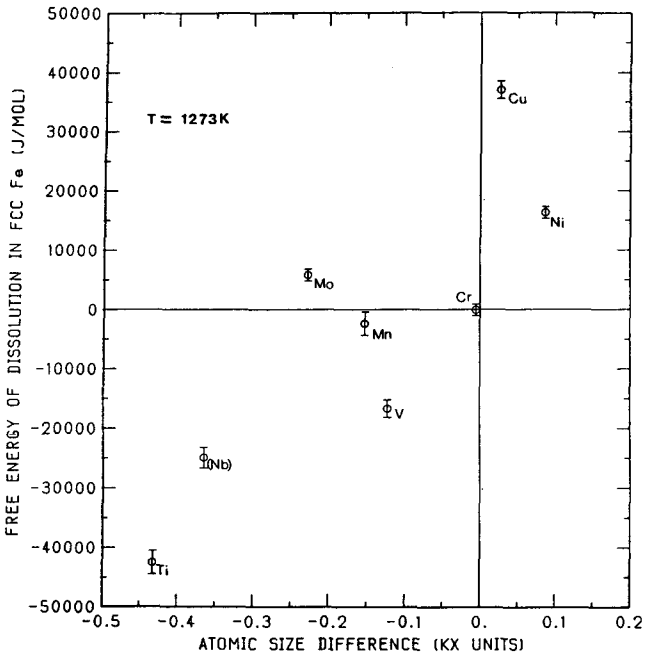


Fig. 16—Correlational relationship: free energy of dissolution of solute in fcc Fe *vs* atomic size difference.

$[(-8030/T) + 3.89]$. The value is composed of three components, namely, (1) the free energy of formation of the stoichiometric carbide,[7] (2) the free energy of dissolution of carbon,[46] and (3) free energy of dissolution of niobium in austenite. The contributions from the first two components are the same in both studies, and therefore, the difference in the solubility expression values must result from different values for the free energy of dissolution of bcc Nb in fcc Fe. The free energies of dissolution ($RT \ln {}^{\circ}\gamma_{Nb}$) determined in these studies are given in Table VIII, along with the solubility limits and the interaction parameters. It can be seen that the ($RT \ln {}^{\circ}\gamma_{Nb}$) values evaluated from the Ohtani *et al.* results are indeed more positive in both cases compared to the value obtained in the present study. This is in line with the solubility differences observed here; *i.e.*, the lower the solubility the more positive is the free energy of dissolution. The complex analysis of this value was in the earlier part of our study,[1] and it was shown that the value obtained here is in relatively good agreement with the values obtained from Fe-Nb-N studies and fulfills well the expected correlational relationships as was shown in Figures 16 and 17.

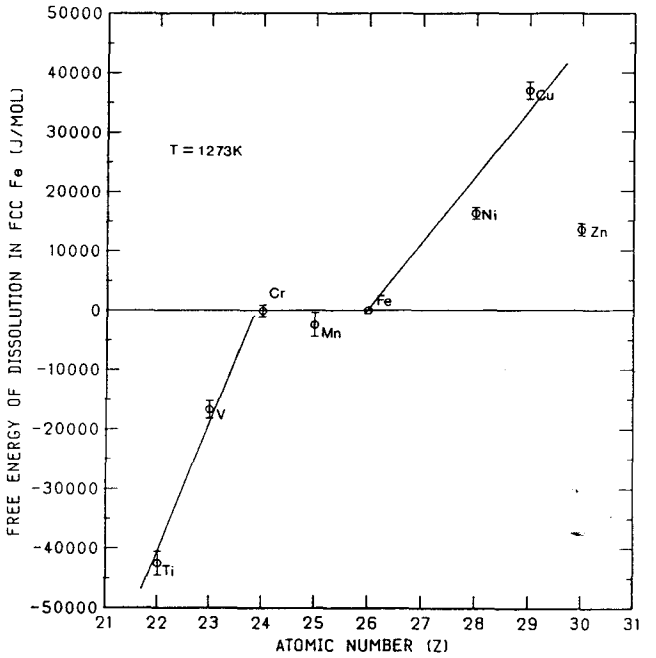


Fig. 17—Correlational relationship: free energy of dissolution of solute in fcc Fe *vs* atomic number of the solute.

The thermodynamic parameters which were used for the calculations of the thermodynamic equilibria in our study and in Ohtani *et al.*'s article[21] show similar relations as the above-mentioned interaction parameters and free energies of dissolution. The value of the $L_{FeNb:C}$ parameter in Ohtani *et al.*'s study is only slightly more negative than ours, corresponding to a more negative value of $\varepsilon_C^{Nb}$, which is displayed in the greater curvature of the phase boundary at higher content of carbon. Ohtani *et al.*'s value of the parameter $L_{FeNb:Va}$ is more positive, especially for the higher temperatures, and shifts the phase boundary toward low contents of niobium. The parameters $L_{CVa:Nb}$ and $L_{CVa:Fe}$ differ only a little or are the same in the two studies and therefore have only a small influence on the shift between the results.

The calculations of the equilibrium phase diagram of the Fe-Nb-C system was also made by Huang.[47] The results in that very complete study show different shapes of the $\gamma/\gamma$ + NbC phase boundary than the results in the present and Ohtani *et al.*'s studies. The solubility of carbide is low in Huang's study (corresponding to a more positive value of the $L_{FeNb:Va}$ parameter (−4784) than in the present study) and no backward bend is displayed for higher contents of carbon, as shown in Figure 13. In Huang's study, the value of $\varepsilon_C^{Nb}$ and the value of the thermodynamic parameter describing the mutual interaction of solutes are evaluated on the basis of the theoretical thermodynamic analysis of available data in literature, and the value of the ternary interaction parameter $\varepsilon_C^{Nb} = -38{,}276/T + 3.1$ is accepted for the calculation. This more positive value does not correspond to the strong mutual interaction observed in our study and in Ohtani *et al.*'s studies. This very careful theoretical analysis of thermodynamic and phase data made by Huang shows clearly that some uncertainty still exists in the description of this system. The analysis made in our study, based on the experimental results, indicates that the reliability of the parameters evaluated is good. The qualitatively similar results obtained in Ohtani *et al.*'s study, especially concerning the tendency of the solubility of carbide to be higher than in Huang's study and the backward bend for the higher content of carbon, give support to the validity of our results. The more complete calculations which were carried out by Ohtani *et al.* in Reference 21 show an acceptable shape for the ternary miscibility gap in the austenite-carbide equilibria, in contrast to Huang's shape, calculated for a very high absolute value of the thermodynamic parameter $L_{FeNb:C}$ (corresponding to $\varepsilon_C^{Nb}$) and similar to that used in our study for the austenite phase.

### A. *Correlational Relationships and the Ternary Interaction Parameters*

It is fairly well established[48] that a regular pattern exists in the crystal structure of carbides and nitrides as one traverses along a period. The tendency to form closed-packed structures as interstitial solutes are added increases as one moves away from iron to the left of the Periodic Table. The group IV and V elements, which exist in bcc and hcp lattices on addition of interstitial solutes, stabilize the fcc phase in the form of a carbide or nitride. To the right of iron, we see Ni, Co, Cu, *etc.*, which already exist in fcc form, and the carbides and nitrides of these elements are mostly unstable. Near iron, we see the transition from bcc metals forming fcc carbides to fcc metals forming unstable carbides and nitrides. Thus, Cr, Mn, and, to some extent, iron itself form complex carbides which exist in orthorhombic, cubic, and hexagonal structures. The periodic pattern in structure is accompanied by the anticipated variation of the free energies of formation of carbides and nitrides, with large negative values for group IV and V compounds changing to positive values for the unstable carbides in group VII and VIII. Since iron lies near the transition, the solutes to the far left form very stable carbides and nitrides (TiC, NbC, *etc.*) and the solutes near iron form complex carbides with iron dissolved ($(Fe,Cr)_3C$, *etc.*) in them.

In an earlier section, we noted the Periodic Table variation of the dissolution free energy of the solutes belonging to the first long period in fcc iron. In this section, we explore the correlational relationships between the ternary interaction parameters and the free energies of formation of carbides. The free energy of formation of a binary compound is one of the indicators of the degree of attraction/repulsion between the two components that make up the compound. The more negative the free energy of formation the higher is the degree of attraction. When the two elements that form the compound are dissolved in a solvent like Fe, depending on the nature and the magnitude of interaction of the individual solutes with the solvent, the one-to-one correspondence between the free energy of formation and the degree of solute interaction will be affected. In the following, the nature and the degree of correlation will be investigated.

Figure 18 illustrates the correlation between the ternary interaction parameters and the free energies of formation of stoichiometric carbides from pure elements as well as from austenite. The free-energy values have been taken from compilations of Hultgren *et al.*[7] and Kubaschewski *et al.*[49] The carbon interaction parameters for Ti, Nb, and V have been taken from the results of Ohtani *et al.*[19,20] and those obtained in the present study. The values for carbon with Ni, Mn, Cr, and Mo have been taken from the compilation by Sharma *et al.*[50] The free energies of formation from austenite have been determined using the dissolution free-energy values listed in Table XII.

From Figure 18, it can be seen that there is a linear variation of the carbon-metal interaction with the free energy of formation from pure elements. This implies that the interaction of the solutes in fcc iron is very similar to the interaction between these elements in the carbide. This striking linear correlation is somewhat lost if we instead consider the free energy of formation from austenite. The dissolution free energies of transition metal solutes in the fcc form in fcc Fe (Figure 17) vary fairly linearly, but the lattice stability of solutes (free-energy difference between the fcc and bcc forms) varies in a nonlinear way with group number. Therefore, the combination of these energies which is used in the calculation of the free energy of formation from austenite varies nonlinearly. However, two groups of solutes can be identified, those that form cubic carbides (group IV and V) and others that form hexagonal, orthorhombic carbides (Cr, Mn, W, Mo, *etc.*), and a fairly good correlation exists within each group.

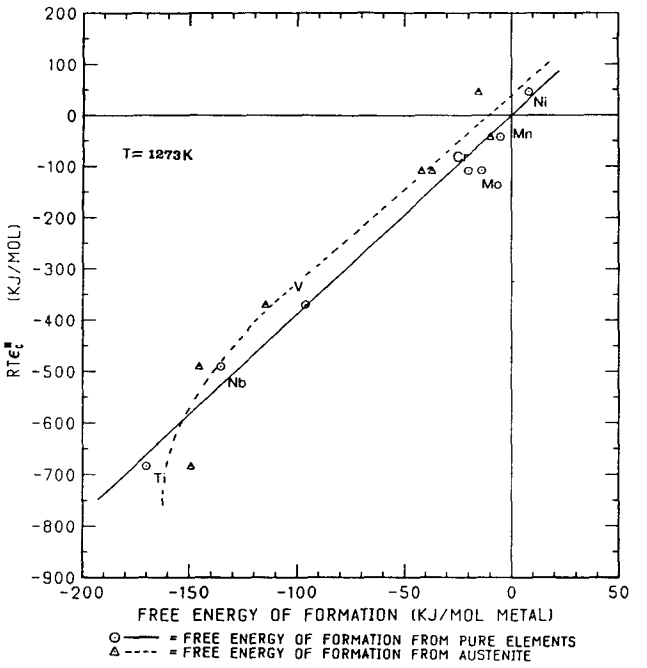


Fig. 18—Correlational relationship: carbon-metal interaction parameter in austenite *vs* free energy of formation of carbide.

## VII. SUMMARY

The thermodynamics of Fe-Nb-C austenites and the solubility of niobium carbide have been investigated using a dynamic gas equilibration technique together with a Cahn microbalance for determining the carbon contents *via* dynamic weight change measurements in the temperature range of 1273 to 1473 K.

1. The solubility limit of the carbide determined as the change of slope in the variation of carbon content with titanium additions shows a minimum between 0.4 and 0.5 wt pct C in the temperature range of 1273 to 1473 K.
2. The increase in the carbon content has been used to determine the niobium-carbon interaction in the modified Wagner formalism as

$$\varepsilon_C^{Nb} = -\frac{(65{,}350 \pm 4000)}{T} + (2.5 \pm 2)$$

3. The variable solubility limit of niobium carbide at high carbon levels was described using an additional term dependent on the ternary interaction parameter, as in the case of solubility of TiC in Fe-Ti-C austenite. The solubility of NbC is determined as

$$\log [(\text{wt pct Nb})\ (\text{wt pct C})] = [-(8030/T) + 3.89] + [(1150/T) - 0.05]\ \text{wt pct C}$$

4. The dissolution free energy of bcc Nb in fcc Fe determined from the various solubility investigations has been analyzed. Periodic Table variation of the dissolution free energies and the consistency in the values obtained from various investigations on the solubility of NbC and NbN in their respective austenites have been used as the criteria in the assessment of the values for bcc Nb in fcc iron. The recommended average value is

$$RT \ln {}^{\circ}\gamma_{Nb} = -25{,}500 + 10.9T \quad \text{Joules/mol Nb}$$

5. The sublattice-subregular model has been used for the description of the thermodynamics of austenite and the NbC and TiC phases. The results from the gas equilibration experiments on $NbC_y$ and austenite, along with the data available in the literature, have been analyzed and the interaction parameters in the model determined. The data on $TiC_y$ phase are described satisfactorily by the parameters obtained by Kaufman and Agren.[15] The calculations made with these parameters yield very good agreement with the experimental results.

## REFERENCES


1. K. Balasubramanian, A. Kroupa, and J.S. Kirkaldy: *Metall. Trans. A*, 1992, vol. 23A, pp. 709-27.
2. M. Hillert and L.I. Staffansson: *Acta Chem. Scand.*, 1970, vol. 24, pp. 3618-26.
3. J. Sopousek and A. Kroupa: *Res. Rep. VZ882/961*, Institute of Physical Metallurgy, Brno, Czechoslovakia, 1991.
4. S.D. Conte and C. de Boor: *Elementary Numerical Analysis—An Algorithmic Approach*, 3rd ed., McGraw-Hill, New York, NY, 1980, ch. 6, sections 6.1–6.4.
5. E.K. Storms, B. Calkin, and A. Yencha: *High Temp. Sci.*, 1969, vol. 1, p. 430.
6. Y.R. Hong, R.V. Kumar, K. Balasubramanian, and D.A.R. Kay: McMaster University, Hamilton, ON, Canada, unpublished research, 1987.
7. R. Hultgren, P. Desai, D.T. Hawkins, M. Gleiser, and K.K. Kelly: *Selected Values of the Thermodynamic Properties of Binary Alloys*, ASM, Metals Park, OH, 1973, pp. 503 and 520.
8. L. Kaufman and H. Nesor: *CALPHAD*, 1978, vol. 2, pp. 55-63 and 117.
9. V.I. Alekseev, A.S. Panov, Ye.V. Fiveiskii, and L.A. Shvartsman: *Proc. Thermodynamic of Nuclear Materials 1967*, IAEA, Vienna, 1968, pp. 435-47.
10. P. Grieveson: *Proc. British Ceram. Soc.*, 1967, vol. 8, pp. 137-53.
11. V.I. Malkin and V.V. Pokidshev: *Russ. J. Phys. Chem.*, 1971, vol. 45, pp. 1159-61.
12. K. Koyama and Y. Hasimoto: *Nippon Kinzoku Gakkai-si*, 1973, vol. 37, pp. 406-11.
13. E.K. Storms: *Refractory Carbides*, Academic Press, New York, NY, 1967, pp. 16-17.
14. F. Tessandier, M. Ducarrior, and C. Bernard: *CALPHAD*, 1989, vol. 8, p. 233.
15. L. Kaufman and J. Agren: Tech. Rep. F49620-80-C-0020, Air Force Office of Scientific Research (AFSC), Bolling Air Force Base, Washington, DC, 1982.
16. B. Uhrenius: *CALPHAD*, 1984, vol. 8, p. 101.
17. P. Gustafson: *Scan. J. Met.*, 1985, vol. 14, pp. 259-67.
18. W. Huang: *Mater. Sci. Technol.*, 1990, vol. 6, pp. 687-94.
19. H. Ohtani, T. Nishizawa, T. Tanaka, and M. Hasebe: *Proc. Japan-Canada Seminar on Secondary Steelmaking*, Tokyo, The Canadian Steel Industry Research Association (CSIRA) and The Iron and Steel Institute of Japan (ISIJ), 1985, pp. J-7-1-J-7-12.
20. T. Nishizawa, H. Ohtani, and M. Hasebe: Presentation, *CALPHAD XIV*, Boston, MA, 1985.
21. H. Ohtani, M. Hasebe, and T. Nishizawa: *CALPHAD*, 1989, vol. 13, pp. 183-204.
22. K. Balasubramanian and J.S. Kirkaldy: *CALPHAD*, 1986, vol. 10, pp. 187-202.
23. E. Paul and L.J. Swartzendruber: *Bull. Alloy Phase Diagrams*, 1986, vol. 7, p. 286.
24. R.J. Hawkins: *Symp. on Chemical Metallurgy of Iron and Steel*, British Steel Corporation (BSC) Corporate Laboratories—University of Sheffield, Iron and Steel Inst./The Metal Society, London, 1973, p. 310.
25. F. deKazinsky, A. Axnas, and P. Pachleiter: *Jernkontorets Ann.*, 1963, vol. 147, p. 408.
26. T. Mori: *Tetsu-to-Hagané*, 1964, vol. 50, p. 911.
27. K. Narita and S. Koyama: *J. Jpn. Inst. Met.*, 1966, vol. 52, p. 292.
28. L. Meyer: Dissertation, Clausthal Berg., Hulten, 1966; *Z. Metallkd.*, 1967, vol. 58, pp. 334-39.
29. R.P. Smith: *Trans. TMS-AIME*, 1966, vol. 236, p. 220.
30. T.H. Johansen, N. Christensen, and B. Auglan: *Trans. TMS-AIME*, 1967, vol. 239, p. 1651.
31. S. Koyama: *J. Jpn. Inst. Met.*, 1972, vol. 52, p. 1090.
32. T. Mori, M. Tokizane, and K. Yanaguchi: *Tetsu-to-Hagané*, 1968, vol. 54, p. 763.
33. R.P. Smith: *Trans. TMS-AIME*, 1962, vol. 224, p. 190.
34. K. Narita: *J. Chem. Soc. Jpn.*, 1956, vol. 77, p. 1536.
35. K. Balasubramanian: Ph.D. Thesis, McMaster University, Hamilton, ON, Canada, 1988.
36. W. Hume-Rothery: *Structures of Alloys of Iron*, Pergamon Press, New York, NY, 1966, ch. 5.
37. G. Kirchner, H. Harvig, K.R. Moguist, and M. Hillert: *Arch. Eisenhuttenwes.*, 1973, vol. 44, p. 227.
38. Z. Moser, W. Zakulski, P. Spencer, and H. Hack: *CALPHAD*, 1985, vol. 10, p. 259.
39. A. Jansson: Internal Report No. TRITA-MAC-0340, Royal Institute of Technology, Stockholm, Sweden, 1985.
40. S. Hertzman and Bo Sundman: Internal Report No. TRITA-MAC-0243, Royal Institute of Technology, Stockholm, Sweden, 1984.
41. J.O. Anderson and Bo Sundman: TRITA-MAC-0270, Royal Institute of Technology, Stockholm, Sweden, 1986.
42. J.O. Anderson and N. Lange: TRITA-MAC-0322, Royal Institute of Technology, Stockholm, Sweden, 1986.
43. W. Huang: TRITA-MAC-0309, Royal Institute of Technology, Stockholm, Sweden, 1986.
44. J.O. Anderson: *CALPHAD*, 1983, vol. 7, pp. 295-305.
45. J.L. Murray: *Bull. Alloy Phase Diagrams*, 1981, vol. 2, pp. 320-34.
46. J. Chipman: *Metall. Trans.*, 1972, vol. 3, pp. 55-64.
47. W. Huang: *Zeit. Für Metall.*, 1990, vol. 81, pp. 397-404.
48. H.J. Goldschmidt: *Interstitial Alloys*, Plenum Press, New York, NY, 1967, Sections 2.5 and 4.1, pp. 44-46 and 88-101.
49. O. Kubaschewski, E.LL. Evans, and C.B. Alcock: *Metallurgical Thermochemistry*, 4th ed., Pergamon Press, New York, NY, 1967, pp. 421-29.
50. R.C. Sharma, V.K. Lakshmanan, and J.S. Kirkaldy: *Metall. Trans. A*, 1984, vol. 15A, pp. 545-53.
51. *A Handbook of Lattice Spacings and Structures of Metals and Alloys*, W.B. Pearson, ed., Pergamon Press, New York, NY, 1985, p. 21 and Table 7.